How Does Ammonium Interact with Aromatic Groups? A Density Functional Theory (DFT/B3LYP) Investigation

ARTICLE *in* THE JOURNAL OF PHYSICAL CHEMISTRY A · OCTOBER 2000

Impact Factor: 2.69 · DOI: 10.1021/jp001306v

10 AUTHORS, INCLUDING:

Weiliang Zhu
Shanghai Institute of Materia Medica
209 PUBLICATIONS **3,915** CITATIONS

SEE PROFILE

Joel Sussman
Weizmann Institute of Science
359 PUBLICATIONS **22,802** CITATIONS

SEE PROFILE

How Does Ammonium Interact with Aromatic Groups? A Density Functional Theory (DFT/B3LYP) Investigation

Wei-Liang Zhu,[†,‡] Xiao-Jian Tan,[‡] Chum Mok Puah,*[,†] Jian-De Gu,[‡] Hua-Liang Jiang,*[,‡,§] Kai-Xian Chen,[‡] Clifford E. Felder,[§] Israel Silman,[||] and Joel L Sussman*[,§]

Chemical Process and Biotechnology Department, Singapore Polytechnic, 500 Dover Road, Singapore 139651, State Key Laboratory of Drug Research, Shanghai Institute of Materia Medica, Shanghai Institutes for Biological Sciences, Chinese Academy of Sciences, 294 Taiyuan Road, Shanghai 200031, P. R. China, and Departments of Structural Biology and Neurobiology, Weizmann Institute of Science, 76100 Rehovot, Israel

Received: April 4, 2000; In Final Form: July 5, 2000

DFT/B3LYP calculations were carried out on complexes formed by NH_4^+ with aromatics, viz. benzene, phenol, pyrrole, imidazole, pyridine, indole, furane, and thiophene, to characterize the forces involved in such interactions and to gain further insight into the nature and diversity of cation−aromatic interactions. Such calculations may provide valuable information for understanding molecular recognition in biological systems and for force-field development. B3LYP/6-31G** optimization on 35 initial structures resulted in 11 different finally optimized geometries, which could be divided into three types: $NH_4^+-\pi$ complexes, protonated heterocyclic−NH_3 hydrogen bond complexes, and heterocyclic−NH_4^+ hydrogen bond complexes. For $NH_4^+-\pi$ complexes, NH_4^+ always tilts toward the carbon−carbon bond rather than toward the heteroatom or the carbon−heteroatom bond. The calculated CHelpG charges suggest that the charge distribution of a free heterocyclic may be used to predict the geometry of its complex. Charge population and electrostatic interaction estimations show that the $NH_4^+-\pi$ interaction has the largest nonelectrostatic interaction fraction (∼47%) of the total binding energy, while the NH_4^+−aromatic hydrogen bond interaction has the largest electrostatic fraction (∼90%). A good correlation between binding energy and electrostatic interaction in the $NH_4^+-\pi$ complexes is found, which shows that nonelectrostatic interaction is important for cation−π binding. The results calculated with basis sets from 6-31G to 6-311++G(2df, 2dp) show that ΔE^{corr} and ΔH^{corr} do not require a basis-set superposition error (BSSE) correction, in view of experimental error, if a larger basis set is used in the calculation. The calculated ΔH^{corr} values for the $NH_4^+-C_6H_6$ complex with different basis sets suggest that the experimental ΔH may be overestimated.

Introduction

Extensive experimental and theoretical investigations in the past decade have revealed that the interaction between cations and aromatic groups, the cation−π interaction, plays an important role in biological processes.[1−5] Such interactions may be several times stronger than other noncovalent interactions, such as hydrogen bonding and hydrophobic interactions.[4] Thus, they may be important in molecular recognition, drug action, and protein-folding. Recently, Dougherty and co-workers used energy-based criteria to search a protein database composed of 593 proteins. They found that over 25% of all tryptophans in their database experience an energetically significant cation−π interaction.[6] Thus the cation−π interaction is indeed prevalent in biomacromolecules. A detailed understanding of this interaction might, therefore, be helpful in evaluating its biological significance, in designing new drugs and engineering modified proteins as well as in developing improved molecular force fields.

Our interest in cation−π binding stems from our efforts to design new enzyme inhibitors and channel blockers that selectively interact with acetylcholinesterase (AChE) and with potassium ion channels (PICs), respectively, with the eventual aim of developing new drugs for the treatment of Alzheimer's disease (AD) and cardiovascular diseases. In both these systems, cation−π interactions play an important role.[7−11] The X-ray structures of various AChE-inhibitor complexes clearly indicate that the cation−π interaction is essential for ligand binding.[5,7,8,11−15] Site-directed mutagenesis and, more recently, X-ray crystallography have shown the importance of cation−π interactions in PICs.[9−10]

However, to the best of our knowledge, and unlike other enzyme targets such as HIV-1 protease,[16] no new lead compounds for AChE inhibitors or for PIC blocking agents have been found with the use of the available structure-based drug design (SBDD) methods such as DOCK.[17] One reason may be that such drug-design and molecular modeling methods are based on a simplified set of interatomic interactions, which do not include the cation−π interaction between ligands and proteins containing aromatic-rich binding sites. Thus, development of improved force fields, capable of reproducing the interactions between cation and aromatics, is a task of top priority.

Theoretical investigations are an excellent complement to experimental studies on cation−π interactions. Numerous quantum chemistry studies have been carried out, focusing

* Corresponding authors. Please address correspondence and requests for reprints to: Prof. Hua-Liang Jiang, Shanghai Institute of Materia Medica, Chinese Academy of Sciences, 294 Taiyuan Road, Shanghai 200031, P. R. China. Phone, +86-21-64311833, ext. 222; fax, +86-21-64370269; e-mail, jiang@iris3.simm.ac.cn or hljiang@mail.shcnc.ac.cn.

[†] Singapore Polytechnic.

[‡] Chinese Academy of Sciences.

[§] Department of Structural Biology, Weizmann Institute of Science.

[||] Department of Neurobiology, Weizmann Institute of Science.

10.1021/jp001306v CCC: $19.00
Published on Web 10/03/2000

especially on the electronic and geometrical structures of cation−π complexes.[4,18−24] The calculated results are, in general, in agreement with the experimental results.

Like other noncovalent interactions, cation−π binding can be divided into two parts: electrostatic and nonelectrostatic, including polarization, dispersion, and charge transfer.[4,25] Dougherty found that if one simply wants to predict the trend in a cation−π interaction across a series of aromatics, one need only consider electrostatics.[4] In particular, an excellent correlation was found between the self-consistent field (HF/6-31G**) binding energies and the molecular electrostatic potential (MEP) for a series of 11 derivatives of benzene.[26] However, it was also found that the fraction of the total binding energy that is electrostatic varies from 60 to 0%, depending on the aromatic core.[4,26] The Cubero group performed a quantum mechanical study on the polarization contribution to cation−π interactions using the GMIPp (Generalized Molecular Interaction Potential with Polarization) method, which showed the importance of the polarization contribution that explains most of the "missed energy term" in Dougherty's correlations.[25]

We performed calculations earlier for some model systems in which ammonium (NH_4^+) was complexed with four nitrogen-containing heterocyclic aromatics at the B3LYP/6-31G* level, so as to investigate their geometry characteristics and thermodynamic parameters, without considering either the basis-set superposition error (BSSE) or the zero-point vibrational energy (ZPVE).[20] This study demonstrated that other interactions exist in cation−aromatic systems, in addition to the cation−π interaction. To address the diversity of interactions between cations and aromatics, and as a first step toward force-field parametrization of cation−aromatic interactions, various geometrical and thermodynamic parameters are needed. In the following, we present a comprehensive density functional theory (DFT) study of cation-aromatic interactions between ammonium and eight aromatics, namely benzene, phenol, pyrrole, imidazole, pyridine, indole, furane, and thiophene. To the best of our knowledge, although limited studies for the complexes of NH_4^+-benzene, NH_4^+-phenol, and NH_4^+-indole have been carried out,[4,18−24,27] no systematic analysis of this type has been made using a sophisticated quantum chemical method. Our objective was not only to determine the geometries and thermodynamic parameters of the complexes formed by NH_4^+ with these eight unsubstituted aromatics, but also to gain further insight into the nature and diversity of cation−aromatic interactions, which, as mentioned, may provide valuable information for understanding molecular recognition in biological systems and for developing force field. We also paid close attention to the contributions of electrostatic and nonelectrostatic interactions to the total binding energy. To accomplish these goals, we also estimated BSSE and ZPVE terms. In addition, different basis sets from 6-31G to 6-311++G(2df, 2pd) were used to investigate the effect of the basis set on BSSE and ZPVE.

Computational Details. Density functional theory has recently been recognized as an efficient quantum chemistry method for studying molecular properties.[28] Our previous studies, using the B3LYP[29] method with different basis sets, showed that DFT provides a satisfactory tool to investigate cation−π interactions, especially to make thermodynamic, geometry, and vibrational spectrum calculations in comparison with MP2 and experimental results.[19−23] Hence, the DFT/B3LYP method was employed throughout this study.

We designed 35 possible initial structures for NH_4^+−aromatic complexes, so as to obtain the real minimum energy structures (Figure 1). These initial structures could be broadly divided into two types: cation−π complexes and hydrogen-bond complexes. In the case of NH_4^+−π complexes, the NH_4^+ was located above the plane of the aromatic ring, with one, two, or three hydrogen atoms directed toward the ring. These hydrogen atoms might tilt toward either a heteroatom or a carbon atom. The B3LYP/6-31G* method was employed for full optimization of these initial structures. The optimized structures were then subjected to further optimization with B3LYP/6-31G**, followed by frequency calculations to verify the reasonability of the optimized structures and to determine the thermal energy, ZPVE, and entropies. After that, BSSE and electrostatic interaction calculations were performed on the basis of optimized geometries. BSSE was estimated by use of the following equation:[30]

$$\mathrm{BSSE} = [E_A - E_{A(AB)}] + [E_B - E_{B(AB)}] \quad (1)$$

where $E_{A(AB)}$ (or $E_{B(AB)}$) is the energy of fragment A (or B), based on the geometry extracted from the optimized structure, with its own basis set augmented by the basis set of B (or A). E_A (or E_B) is the energy of isolated fragment A (or B), with just its own basis set. Estimates of the electrostatic interaction were obtained on the basis of

$$E_{ele} = E_{charge} - (E^0 + E_{self}) \quad (2)$$

Here, E_{charge} is the energy using CHelpG atomic charges[31] located at the atomic nuclei of the cationic atoms, E^0 is the energy without CHelpG charges, and E_{self} is the self-energy of the CHelpG charges. Hence, E_{ele} is the electrostatic energy in a broad sense, which includes all interactions between aromatics and the positive charges of ammonium.

All B3LYP/6-31G* calculations were carried out using Gaussian94[32] software on a Power Challenger R-10000 supercomputer. All B3LYP/6-31G** calculations, including BSSE and electrostatics, were performed using Gaussian98 software[32] on the same computer. Molecular modeling was carried out on an SGI workstation using the SYBYL6.2 software package.[33]

Results and Discussion

Geometries. Figure 2 depicts the B3LYP/6-31G** optimized geometries, which show that three types of complexes are formed between NH_4^+ and the aromatics: NH_4^+−aromatic cation−π complexes, aromatic−NH_4^+ hydrogen-bond complexes, and protonated heterocyclic−NH_3 hydrogen-bond complexes, in which proton transfer occurs from NH_4^+ to the heterocyclic aromatic. For benzene, pyrrole, and indole, the binding product is only the cation−π complex. For imidazole and pyridine, the final result is only the protonated heterocycle−NH_3 hydrogen-bond complex, no matter what initial structures are used during the geometry optimization. With respect to phenol, furane, and thiophene, the binding complexes could be categorized as either NH_4^+−π or aromatic−NH_4^+ hydrogen-bond complexes. These optimized geometries suggest that the energetically favorable interaction model of cationic ligands, such as the protonated side chains of lysine and arginine, with phenylalanine or tryptophan, is a cation−π interaction. Energetically, a hydrogen-bond interaction is the most probable interaction model of these cationic ligands with the side chain of histidine at physiological pH, accompanied by proton transfer from the protonated amino group to the aromatic ring. Both hydrogen-bond and cation−π interactions are possible between these cationic ligands and tyrosine. The optimized geometries also suggested that both cation−π and hydrogen-bond interactions are possible between these groups and the heterocyclic aromatics, furane and thiophene. However, hydrogen-bond

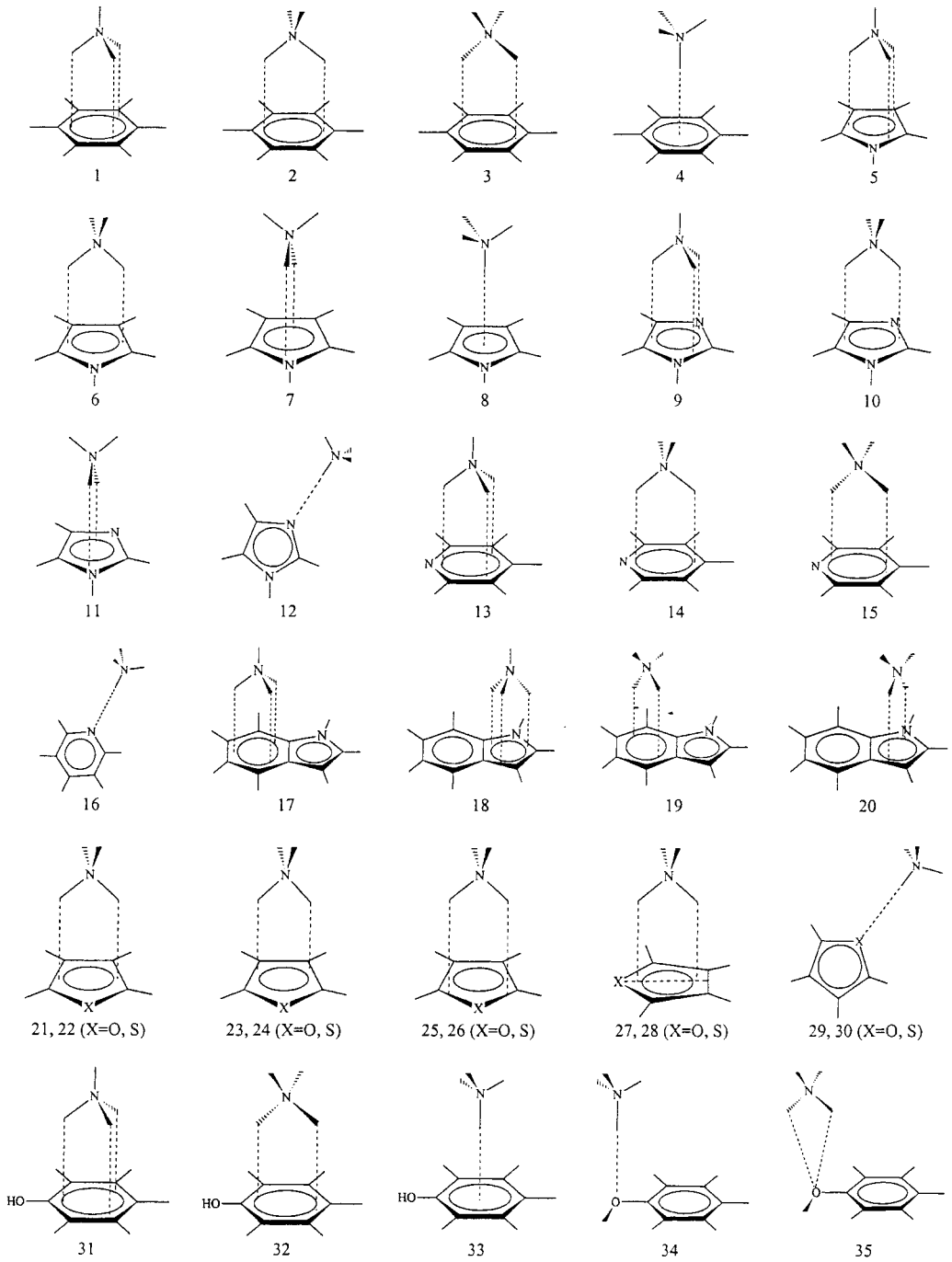

Figure 1. Thirty-five initial structures of the complexes constructed from NH_4^+ and eight different aromatics.

binding is the most probable interaction between such cations and pyridine.

Table 1 summarizes some distances between the H of NH_4^+ and the aromatic rings in the $NH_4^+-\pi$ complexes. The perpendicular distances, r_2 in Figure 2, are about 2.1 Å between NH_4^+ and nitrogen heterocyclics and phenol, about 2.2 Å between NH_4^+ and oxygen- and sulfur-containing heterocyclics, and 2.3 Å between NH_4^+ and benzene. They are always a little shorter than at the B3LYP/6-31G* level by 0.01 to 0.10 Å (Table 1), suggesting that adding the polarization function to the basis set results in a decrease in the interaction distance. All the distances are rather short for a noncovalent intermolecular interaction, suggesting that the $NH_4^+-\pi$ interaction is quite strong. They also show that, among the cation$-\pi$ complexes, NH_4^+-nitrogen heterocyclic interactions are most probably the strongest, because the distances calculated for them are the shortest (Table 1). The projection of the H of NH_4^+ on the aromatic ring plane is always closer to the carbon atoms than to the heteroatoms. Furthermore, the projection is always nearer to the carbon−carbon rather than to the carbon−heteroatom bond (Figure 2).

Table 2 presents the hydrogen-bond lengths of the hydrogen-bond complexes. They range from 1.6 to 1.7 Å, except for the NH_4^+-thiophene hydrogen-bond complex, for which the value is 2.23 Å. The distances between the two heavy atoms participating in these hydrogen bonds are 2.6−2.8 Å, except in the NH_4^+-thiophene hydrogen-bond complex, for which the value is 3.28 Å. A slight decrease in hydrogen-bond length is observed after a polarization function is added to B3LYP/6-31G*. In all these complexes, except the NH_4^+-thiophene

TABLE 1: Distances (Å) between NH_4^+ and Aromatic Groups in Cation−π Complexes

		NH_4^+−benzene	NH_4^+−phenol	NH_4^+−pyrrole	NH_4^+−indole	NH_4^+−furane	NH_4^+−thiophene
6-31G*	r_1[a]	2.4434	2.2997	2.0989	2.2057	2.3585	2.3129
	r_2	2.3910	2.1934	2.0460	2.0996	2.3216	2.2303
6-31G**	r_1[b]	2.4358	2.1842	2.0621	2.1938	2.2718	2.2985
	r_2	2.3221	2.1021	2.0101	2.0893	2.2284	2.2149

[a] r_1: The nearest distance between the H of NH_4^+ and the heavy atom of the aromatic. [b] r_2: The perpendicular distance between the H of NH_4^+ and the aromatic plane.

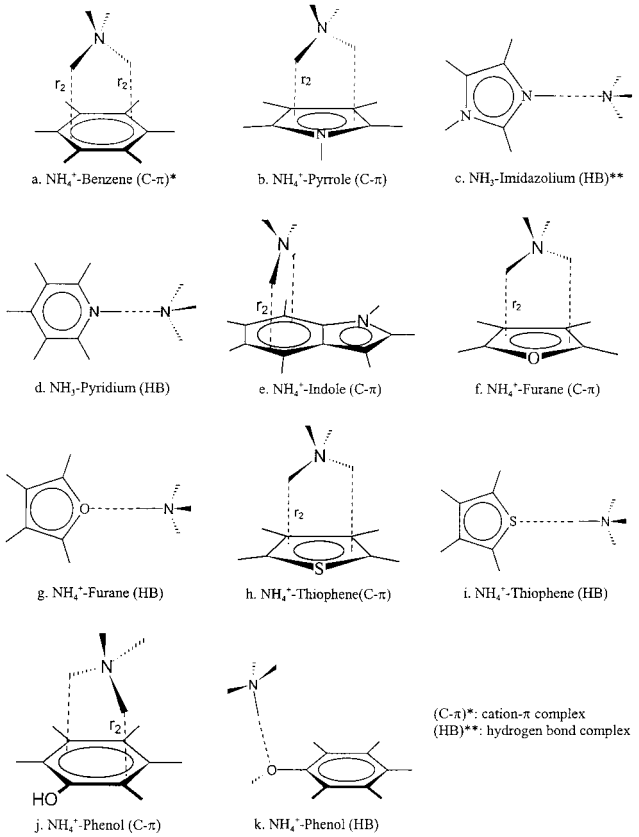

Figure 2. Optimized structures of the complexes formed by NH_4^+ and eight different aromatics at the B3LYP/6-31G** level.

complex, the distances are quite short compared with usual hydrogen-bond lengths, indicating that these hydrogen bonds are unusually strong.

Our optimized geometries also indicate that in all NH_4^+−π complexes, the N−H bonds of NH_4^+ that face the aromatics are 0.01−0.03 Å longer than in free NH_4^+, suggesting that the interaction between NH_4^+ and the aromatic ring weakens these bonds. The calculated bond angles also show that complexation results in the hydrogen atoms of the aromatics bending out of the plane of the ring, and moving away from NH_4^+; the out-of-plane angles range from 2 to 6°. This may be due to repulsion between these hydrogens and NH_4^+. However, the dihedral angles of the ring hydrogens do not change significantly in the hydrogen-bond complexes. This may be due to the lateral binding of the two fragments.

Charge Population Analysis. CHelpG charges[31] were calculated at the B3LYP/6-31G** level on the optimized structure. We divided the complexes into two parts, aromatic and NH_4^+/NH_3, to investigate possible charge transfer between them during complex formation. Table 3 summarizes the sum of total atomic charges of these two parts for each complex. It is clear that the single unit of positive charge is delocalized onto the two parts in all complexes, suggesting that NH_4^+−aromatic interaction is accompanied by charge transfer.

For cation−π complexes, the positive charge is obviously still distributed mainly on the NH_4^+ side. Among all the cation−π complexes, charge transfer was strongest for the NH_4^+−indole pair, and weakest for the NH_4^+−furane pair, suggesting that binding between NH_4^+ and indole is the strongest in the series, and between NH_4^+ and furane the weakest. As might be predicted, in the NH_4^+−aromatic hydrogen-bond complexes, most of the unit charge is located on the NH_4^+, whereas in the protonated heterocyclic−NH_3 hydrogen-bond complexes, most of the positive charge is located on the protonated aromatics (Table 3).

Our previous calculation at the 6-31G* basis set level revealed that the protonated heterocyclic−NH_3 hydrogen-bond complex is the energetically favorable product if the heteroatom has localized lone-pair electrons.[20] The calculated results at the B3LYP/6-31G** level for nitrogen-containing heterocyclic complexes (see Figure 2) are in agreement with this conclusion. However, for the oxygen- and sulfur-containing heterocyclic complexes, the calculated results show that there is no tendency for proton transfer to occur between NH_4^+ and these heterocyclics, even if they also have localized lone-pair electrons. Thus, the products for oxygen- and sulfur-containing heterocyclics are NH_4^+−aromatic hydrogen-bond complexes (Figure 2g,i). The reason for this is unclear, and further theoretical and experimental studies are required.

As Table 3 shows, the amount of transferred charge in NH_4^+−π complexes is larger than in hydrogen-bond complexes. Thus electron transfer plays a more important role in NH_4^+−π complexes than in hydrogen-bond complexes. This conclusion is discussed more quantitatively in the Electrostatic Interactions section.

Figure 3 depicts the CHelpG charge distribution on free aromatics. Regarding NH_4^+−π complexes, the projection of the H of NH_4^+ onto the aromatic plane is near to that carbon atom with the most negative charge, except in the case of furane (Figure 2a,b,e,f,h, and j; and Figure 3a,b,e−h). In addition, the two carbon atoms of the double bond near the H of NH_4^+ are always negatively charged in NH_4^+−π complexes (Figure 3a,b,e−h). However, the two atoms of each carbon−carbon bond in free imidazole and pyridine bear opposite charges (Figure 3c,d). Hence, the charge distribution of a free aromatic may have an intrinsic effect on the final geometry of the complex formed with NH_4^+.

Thermodynamic Parameters. Table 4 presents the calculated thermodynamic parameters at the B3LYP/6-31G** level, including the change of internal energy, ΔE_{inter}; the thermal energy, $\Delta E_{thermal}$; the entropy, ΔS; and the enthalpy of formation, ΔH. Obviously, ΔE_{inter} and ΔH for protonated heterocyclic−NH_3 hydrogen bond complexes are much larger than for other complexes. Using protonated heterocyclics and NH_3 as the reactants, we estimated the changes of internal energy as 25.117 and 25.312 kcal/mol for NH_3−imidazolium and NH_3−pyridinium complexes, respectively. These results suggest that binding of NH_3 to these two protonated nitrogen heterocyclics is very strong.

TABLE 2: Distances (Å) in Hydrogen-Bond Complexes Formed by NH_4^+ and Aromatics

		NH_4^+−phenol	NH_3−imidazolium	NH_3−pyridinium	NH_4^+−furane	NH_4^+−thiophene
6-31G*	*R*1[a]	1.6079	1.6757	1.6909	1.6750	2.2480
	*R*2[b]	2.6727	2.7591	2.7724	2.7403	3.2970
6-31G**	*R*1	1.5592	1.6469	1.6660	1.6313	2.2293
	*R*2	2.6353	2.7361	2.7518	2.7008	3.2777

[a] *R*1: Hydrogen-bond length. [b] *R*2: The distance between two heavy atoms of a hydrogen bond.

TABLE 3: Sum of Atomic CHelpG Charges (Q/e) at the B3LYP/6-31G Level**

a. Cation−π Complexes Formed by NH_4^+ and Aromatics

	NH_4^+−benzene	NH_4^+−phenol	NH_4^+−pyrrole	NH_4^+−indole	NH_4^+−furane	NH_4^+−thiophene
aromatic	0.265	0.259	0.275	0.291	0.250	0.267
NH_4^+	0.735	0.740	0.725	0.709	0.750	0.733

b. Hydrogen-Bond Complexes Formed by NH_4^+ and Aromatics

	NH_4^+−phenol	NH_3−imidazolium	NH_3−pyridinium	NH_4^+−furane	NH_4^+−thiophene
aromatic	0.157	0.779	0.777	0.158	0.107
NH_4^+/NH_3	0.843	0.221	0.223	0.842	0.893

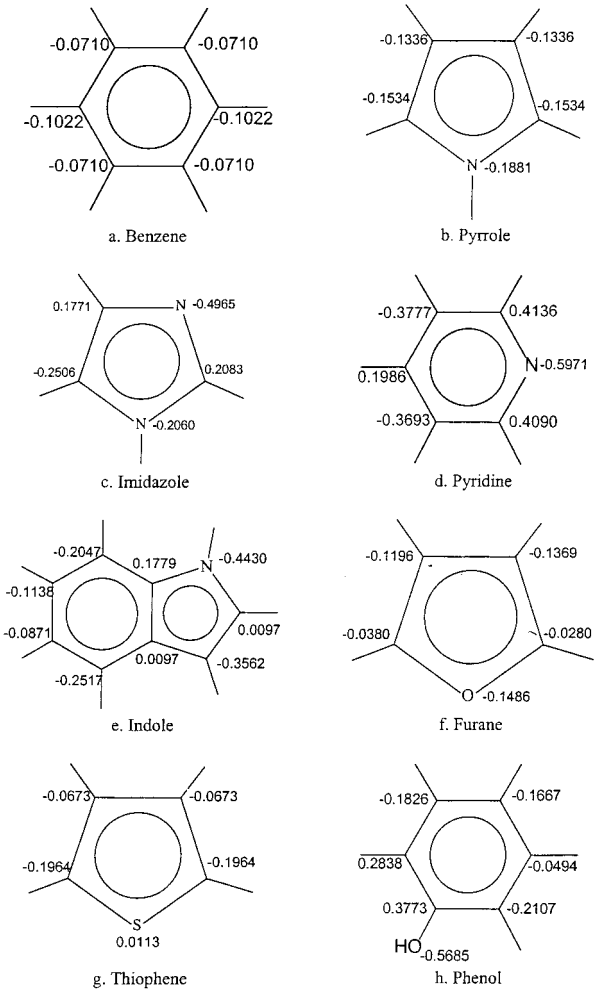

Figure 3. CHelpG charge distribution of free aromatics.

For NH_4^+−π complexes, the nitrogen-containing heterocyclic complexes have the largest thermochemical parameters; the benzene and phenol complexes have intermediate values, and the furane and thiophene complexes have the smallest values (Table 4). Thus the aromatic core affects the binding strength in cation−π complexes significantly. Dougherty and co-workers found that replacing two benzene rings of their synthetic receptor with "electron-rich" furane or thiophene rings led to a decrease in cation binding.[4,34] Our calculated result is consistent with their experimental observation. In addition, our result also shows that thiophene interacts with NH_4^+ more strongly than does furane, by 0.67 kcal/mol. Nevertheless, the hydrogen-bond interaction represents an energetically favorable binding model for furane and NH_4^+ (Table 4). The reason for this is unclear, and further investigation is required.

Deakyne and Meot-Ner[35] utilized the high-pressure mass spectrometer (HPMS) method to determine the binding enthalpy of the NH_4^+−C_6H_6 complex, and they reported a value of 19.3 kcal/mol. Our calculated ΔH is −17.03 kcal/mol, 2.3 kcal/mol less than their experimental value. However, Kim et al.[36] have suggested that the van't Hoff plots of the experimental data may be interpreted as yielding a value of −17.1 kcal/mol, very close to our calculated value.

Because we did not know the effects of BSSE and ZPVE on ΔH, we performed BSSE and ZPVE calculations to correct the values for enthalpy of formation, and these corrected values are also listed in Table 4. The ZPVE ranges from 0.57 to 0.96 kcal/mol, with an average value of 0.81 kcal/mol. In the case of BSSE, the correction is less than 1.0 kcal/mol for NH_4^+−π complexes, but larger than 1.0 kcal/mol for hydrogen-bond complexes, except for the NH_4^+−thiophene complex, which has the smallest BSSE, 0.36 kcal/mol. Comparing the BSSE with the calculated interaction distances (Tables 1, 2, and 4), we find that interaction distance has a substantial effect on BSSE. This effect may be one reason the BSSE of NH_4^+−π complexes is not important to their total binding energy.

Another question arising from the above discussion is whether the basis set has a significant effect on either the BSSE or the ZPVE of the various complexes. To clarify this point, we carried out ZPVE and BSSE correlation calculations on the NH_4^+−C_6H_6 complex using different basis sets, viz. 6-31G, 6-31G(d), 6-31G(d,p), 6-31++G(d,p), 6-311++G(d,p), and 6-311++G-(2df,2dp) (Table 5). It is clear that BSSE has a tendency to decrease as the basis-set scale increases. The 6-31G basis set has the largest BSSE, 0.952 kcal/mol; the 6-311++G(2df, 2pd) basis set has the smallest BSSE, just 0.294 kcal/mol. It is, therefore, better to add diffuse and polarization functions to the basis set if one does not want to estimate BSSE when using B3LYP method to calculate the binding energy or enthalpy for a NH_4^+−π complex.

Calculated values of ΔH^{corr} for the NH_4^+−C_6H_6 complex, taking into account both BSSE and ZPVE corrections, with basis sets from 6-31G to 6-311++G(2df,2pd), are −15.34 to −14.30 kcal/mol (Table 5). These values, on the average, are lower than

TABLE 4: Thermochemical Parameters Obtained from the B3LYP/6-31G Calculations (ΔE, ΔH, ZPVE, and BSSE, kcal/mol; ΔS, cal/mol/K)**

initial system	complex[a]	ΔE_{inter}	$\Delta E_{thermal}$	ΔS	ΔH	ZPVE	BSSE	ΔE^{corr} [b]	ΔH^{corr} [b]	ΔH	E_{ele}	% of ΔE^{corr}
NH_4^+−benzene	CP	−17.499	1.061	−27.339	−17.03	0.797	0.893	−15.809	−15.34	−19.3[c], −17.1[d]	−8.548	54.07
NH_4^+−pyrrole	CP	−22.050	1.462	−30.218	−21.22	0.964	0.964	−20.122	−19.29		−10.510	52.23
NH_4^+−imidazole	HB	−45.871	1.089	−30.506	−45.37	0.848	1.357	−43.666	−43.16		−14.956	65.28[h]
NH_4^+−furane	CP	−15.439	0.873	−33.611	−15.16	0.756	0.962	−13.721	−13.44		−7.450	54.30
	HB	−17.408	1.256	−22.755	−16.74	0.642	1.152	−15.614	−14.95		−13.381	85.69
NH_4^+−thiophene	CP	−16.691	1.515	−28.338	−15.77	0.844	0.817	−15.030	−14.11		−8.170	54.36
	HB	−10.240	0.336	−35.469	−10.47	0.573	0.364	−9.303	−9.53		−8.352	89.78
NH_4^+−pyridine	HB	−42.492	0.655	−35.855	−42.43	0.859	1.491	−40.142	−40.80		−14.710	64.06[i]
NH_4^+−indole	CP	−23.453	1.551	−29.839	−22.49	0.932	0.933	−21.588	−20.62	−25.9[e]	−11.741	54.39
NH_4^+−phenol	CP	−18.553	1.582	−29.876	−17.69	0.957	0.856	−16.740	−15.88	−17.5[f], −18.5[g]	−9.468	56.56
	HB	−22.831	1.186	−28.758	−22.37	0.744	1.312	−20.775	−20.31	−21.7[f], −22.3[g]	−19.571	94.20

[a] CP represents a cation−π complex; HB represents a hydrogen-bond complex. [b] ΔE^{corr}, ΔE corrected for both BSSE and ZPVE; ΔH^{corr}, ΔH corrected for both BSSE and ZPVE. [c] Experimental result, the NBS pulsed high-pressure mass spectrometer (HPMS) method (ref 35). [d] Experimental result (ref 36). [e] MP2/6-31G*//3-21G raw binding energy (ref 27). [f] B3LYP/6-31G*//B3LYP/6-31G* result (ref 19). [g] MP2/6-31G**//MP2/6-31G** result (ref 19). [h] Estimated based on the ΔE^{corr}(−22.912 kcal/mol) from imidazolium and NH_3. [i] Estimated based on the ΔE^{corr}(−22.962 kcal/mol) from pyridinium and NH_3.

TABLE 5: B3LYP Results for the NH_4^+−C_6H_6 Complex Using Different Basis Sets[a]

basis set	6-31G	6-31G(d)	6-31G(d,p)	6-31++G(d,p)	6-311++G(d,p)	6-311++G(2df,2pd)
ΔE_{inter}	−17.025	−17.566	−17.499	−15.738	−15.878	−15.812
$\Delta E_{thermal}$	1.095	1.737	1.061	1.044	1.054	0.576
ΔS	−25.489	−19.259	−27.339	−23.386	−23.509	−28.796
ΔH	−16.522	−16.421	−17.030	−15.286	−15.416	−15.828
ΔG	−8.922	−10.679	−8.879	−8.313	−8.407	−7.243
ZPVE	0.839	0.941	0.797	0.664	0.676	0.752
BSSE	0.952	0.950	0.893	0.327	0.371	0.294
ΔE^{corr}	−15.234	−15.675	−15.809	−14.747	−14.831	−14.766
ΔH^{corr}	−14.731	−14.530	−15.340	−14.295	−14.369	−14.782

[a] Units are kcal/mol except for ΔS, which is cal/mol/K.

the experimental values given by Deakyne and Meot-Ner[35] by ∼4.5 kcal/mol, and lower by ∼2.3 kcal/mol than the same experimental data interpreted by Kim et al.[36] To investigate the possible effect of the optimization process on the final structure of the NH_4^+−C_6H_6 complex and on its ΔH value, we reoptimized its structure from different initial structures, using the 6-31G** basis set. As a result, in addition to the structure depicted in Figure 2a, we found another optimized complex structure in which the NH_4^+ tilts toward the benzene plane, mainly via one of its hydrogen atoms. However, its energy is higher than that of the structure with the geometry depicted in Figure 1, suggesting that the structure in which the two hydrogen atoms interact with benzene equally should be the minimum energy structure (Figure 2a). This result is in accord with other investigators' theoretical results.[4,27,36] Hence, the difference in ΔH between our calculations and the experimental results is not due to our optimized geometry. Recently, Hoyau and co-workers pointed out that binding enthalpies obtained by HPMS or threshold collision-induced dissociation (CID) techniques are normally overestimated by up to 5 kcal/mol.[37] This might also be true for the NH_4^+−C_6H_6 complex, and thus might explain the discrepancy between the experimental and calculated values of ΔH.

Electrostatic Interactions. The calculated E_{ele}, and its contributions to ΔE^{corr}, are also presented in Table 4. Contributions in the range of 52.2−56.6% correspond to the NH_4^+−π complexes; values of 64.1−65.3% correspond to protonated heterocyclic−NH_3 hydrogen-bond complexes; and values of 85.7−94.2% correspond to aromatic−NH_4^+ hydrogen-bond complexes. Thus, binding in the aromatic−NH_4^+ hydrogen-bond complexes is almost purely electrostatic, whereas nonelectrostatic interactions are as important as electrostatic interactions in the NH_4^+−π complexes. This finding is consistent with our discussion in the section on charge population analysis. It is also in agreement with our earlier conclusion, from highest occupied molecular orbital (HOMO) analysis, that binding between NH_4^+ and heterocyclic groups in their NH_4^+−π complexes is related to s−p interactions.[20] To confirm the nature of the interaction in aromatic−NH_4^+ hydrogen-bond complexes, we performed, as an example, a molecular orbital coefficient analysis on the five highest occupied molecular orbitals of the NH_4^+−phenol complex. This analysis reveals that, in contrast to what was found for the NH_4^+−π complex,[20] the 10 largest atomic orbital coefficients in each of these five highest occupied molecular orbitals of the hydrogen-bond complex do not involve any atoms of the NH_4^+ ion. This result supports the conclusion that electrostatic interactions are a dominant component of the binding in NH_4^+−heterocyclic hydrogen-bond complexes.

Table 4 also shows that the more negative the electrostatic interaction energy, the stronger the overall interaction in the NH_4^+−π complexes. By use of the Partial Least-Squares (PLS) method, we examined the correlation between the corrected binding energy at the B3LYP/6-31G** level and the electrostatic interaction for different aromatic core complexes ranging from benzene to thiophene. The correlation equation is $\Delta E^{corr} = 0.492 + 1.896E_{ele}$ ($r^2 = 0.978$, $F = 175.8$, and $s = 0.510$). Dougherty and co-workers found an excellent correlation between self-consistent field (SCF) binding energies and MEPs for 11 derivatives of benzene ($r = 0.991$, slope = 1.01, intercept = 11.6 kcal/mol).[26] Cubero and co-workers showed that GMIPp is a powerful tool for predicting cation-binding of aromatic compounds ($E_{SCF} = -5.0 + 0.984E_{GMIPp}$, $r = 0.995$).[25] The slopes of their corrections are about 1.0. In contrast to their results, our slope, 1.896, indicates the importance of nonelectrostatic interactions in cation−π complexes. Because our correlation is obtained by comparing different aromatic cores,

it could be used to study $NH_4^+-\pi$ complexes formed by different aromatic systems.

Based on determination of the binding affinity of quaternary ammonium cations to macrocyclic and acyclic "phane esters", Roelens and Torriti [38] concluded that the basic driving force is a purely electrostatic attraction between the permanent charge of the cation and the aromatic ring. Here we find that, for NH_4^+-heterocyclic hydrogen-bond complexes, the electrostatic interactions appear to drive the two partners together. For $NH_4^+-\pi$ complexes, if electrostatic interaction is the driving force when the two partners are well-separated, then both electrostatic and nonelectrostatic interactions, such as electron transfer, may play a role when the two partners are close to each other.

Conclusions

We have presented a comprehensive theoretical study of cation−aromatic interactions between NH_4^+ and various aromatic groups by use of the DFT method DFT/B3LYP. Our calculations using basis set 6-31G** reveal the diversity of the binding of NH_4^+ to these aromatics. We find that nitrogen heterocyclics with localized lone-pair electrons tend to react with NH_4^+ to form protonated heterocyclic$-NH_3$ hydrogen-bond complexes. Benzene, pyrrole, and indole tend to form cation$-\pi$ complexes. Phenol, as well as oxygen and sulfur heterocyclics, can produce both $NH_4^+-\pi$ and NH_4^+-aromatic hydrogen-bond complexes. We also find that each of these types of complexes corresponds to different types of CHelpG charge distribution of their aromatics in the free state. The $NH_4^+-\pi$ complex is probably the final product if the two atoms of a carbon−carbon bond of a free aromatic are both negatively charged (CHelpG charges). However, a protonated heterocyclic$-NH_3$ hydrogen-bond complex is formed if the two atoms of each carbon−carbon bond of a free aromatic have opposite CHelpG charges. Our optimized geometries also show that the $NH_4^+-\pi$ complex normally has the longest interaction distance among these three types of complexes.

The calculated results show that the protonated heterocyclic$-NH_3$ hydrogen-bond complexes produce the largest enthalpies of formation (ΔH). For the $NH_4^+-\pi$ complexes, the nitrogen heterocyclic complexes have the largest ΔH, whereas oxygen and sulfur heterocyclic complexes have the smallest values. All the calculated ΔH^{corr} values for the $NH_4^+-C_6H_6$ complex, corrected by both BSSE and ZPVE for the different basis sets, from 6-31G to 6-311++G(2df, 2pd), suggest that experimental ΔH values might be overestimated and should be redetermined. In addition, our results suggest that BSSE may not be needed to correct the binding energy if a basis set including polarization and diffuse functions is used in calculation. The calculated electrostatic interaction results reveal that the binding for hydrogen-bonding complexes is electrostatic in nature. However, the good correlation between ΔE^{corr} and E_{ele} for $NH_4^+-\pi$ complexes demonstrates that nonelectrostatic forces contribute significantly to the $NH_4^+-\pi$ interaction.

The binding diversity and parameters observed in this study should provide valuable information for evaluating interactions between the side chains of cationic residues such as Lys and Arg, and those of aromatic residues such as Trp, Phe, and Tyr, as well as for molecular recognition between cationic ligands and their targets. These results may strengthen our insight into biological processes such as protein-folding and drug−receptor interaction. They will also be useful for force-field parametrization of cation$-\pi$ interactions.

Acknowledgment. We gratefully acknowledge financial support from the National Natural Science Foundation of China (Grant 29725203), the "863" High-Tech Program of China (Grant 863-103-04-01), and the State Key Program of Basic Research of China (Grant 1998051115). This work was also supported by the U.S. Army Medical and Materiel Command under Contract No. DAMD17-97-2-7022, the EU fourth Framework Program in Biotechnology, the Kimmelman Center for Biomolecular Structure and Assembly (Rehovot, Israel), and the Dana Foundation. The generous support of Mrs. Tania Friedman is gratefully acknowledged. I. S. is Bernstein-Mason Professor of Neurochemistry. The quantum chemistry calculations were performed on Power Challenger R-10000 at The Network Information Center, Chinese Academy of Sciences, Beijing, P. R. China, and on an Origin 2000 at the Weizmann Institute of Science, Rehovot, Israel.

References and Notes

(1) Shepodd, T. J.; Petti, M. A.; Dougherty, D. A. *J. Am. Chem. Soc.* **1988**, *110*, 1983.
(2) Dougherty, D. A.; Stauffer, D. A. *Science* **1990**, *250*, 1558.
(3) Dougherty, D. A. *Science* **1996**, *271*, 163.
(4) Ma, J. C.; Dougherty, D. A. *Chem. Rev.* **1997**, *97*, 1303.
(5) Sussman, J. L.; Harel, M.; Frolow, F.; Oefner, C.; Goldman, A.; Toker, L.; Silman, I. *Science* **1991**, *253*, 872.
(6) Gallivan, J. P.; Dougherty, D. A. *Proc. Natl. Acad. Sci. U.S.A.* **1999**, *96*, 9459.
(7) Carlier, P. R.; Chow, E. S.; Han, Y.; Liu, J.; Yazal, J. E.; Pang, Y. P. *J. Med. Chem.* **1999**, *42(20)*, 4225.
(8) Ordentlich, A.; Barak, D.; Kronman, C.; Flashner, Y.; Leitner, M.; Segall, Y.; Ariel, N.; Cohen, S.; Velan, B.; Shafferman, A. *J. Biol. Chem.* **1993**, *268(23)*, 17083.
(9) Doyle, D. A.; Morais, C. J.; Pfuetzner, R. A.; Kuo, A.; Gulbis, J. M.; Cohen, S. L.; Chait, B. T.; MacKinnon, R. *Science* **1998**, *280*, 69.
(10) Heginbotham, L.; MacKinnon, R. *Neuron* **1992**, *8(3)*, 483.
(11) Silman, I.; Harel, M.; Axelsen, P.; Raves, M.; Sussman, J. L. *Biochem. Soc. Trans.* **1994**, *22(3)*, 745.
(12) Axelsen, P.; Harel, M.; Silman, I.; Sussman, J. L. *Protein Sci.* **1994**, *3(2)*, 188.
(13) Kryger, G.; Silman, I.; Sussman, J. L. *Struct. Fold. Des.* **1999**, *7(3)*, 297.
(14) Raves, M. L.; Harel, M.; Pang, Y. P.; Silman, I.; Kozikowski, A. P. *Nat. Struct. Biol.* **1997**, *4(1)*, 57.
(15) Harel, M.; Schalk, I.; Ehret-Sabatier, L.; Bouet, F.; Goeldner, M.; Hirth, C.; Axelsen, P. H.; Silman, I.; Sussman, J. L. *Proc. Natl. Acad. Sci. U.S.A.* **1993**, *90(19)*, 9031.
(16) Wlodawer, A.; Vondrasek, J. *Annu. Rev. Biophys. Biomol. Struct.* **1998**, *27*, 249.
(17) Kuntz, I. D.; Blaney, J. M.; Oatley, S. J. *J. Mol. Biol.* **1982**, *161*, 269.
(18) Pullman, A.; Berthier, G.; Savinelli, R. *J. Comput. Chem.* **1997**, *18*, 2012.
(19) Tan, X.-J.; Jiang, H.-L.; Zhu, W.-L.; Chen, K.-X.; Ji, R. Y. *J. Chem. Soc. Perkin Trans. 2* **1999**, *1*, 107.
(20) Zhu, W.-L.; Jiang, H.-L.; Puah, C. M.; Tan, X.-J.; Chen, K.-X.; Cao, Y.; Ji, R. Y. *J. Chem. Soc., Perkin Trans. 2* **1999**, *11*, 2615.
(21) Zhu, W.-L.; Jiang, H.-L.; Tan, X.-J.; Chen, J. Z.; Zhai, Y. F.; Gu, J.-D.; Lin, M. W.; Chen, K.-X.; Ji, R. Y.; Cao, Y. *Acta Chim. Sinica* **1999**, *57*, 852.
(22) Jiang, H.-L.; Zhu, W.-L.; Tan, X.-J.; Gu, J.-D.; Chen, J. Z.; Chen, K.-X.; Ji, R. Y. *Science in Chinese (Series B)* **1998**, *41(5)*, 535.
(23) Jiang, H.-L.; Zhu, W.-L.; Tan, X.-J.; Chen, J. Z.; Zhai, Y. F.; Liu, D. X.; Zhao, L.; Chen, K.-X.; Ji, R. Y. *Acta Chim. Sinica* **1999**, *57*, 860.
(24) Minox, H.; Chipot, C. *J. Am. Chem. Soc.* **1999**, *121*, 10366.
(25) Cubero, E.; Luque, F. J.; Orozco, M. *Proc. Natl. Acad. Sci. U.S.A.* **1998**, *95*, 5976.
(26) Mecozzi, S.; West, A. P., Jr.; Dougherty, D. A. *J. Am. Chem. Soc.* **1996**, *118*, 2307.
(27) Basch, H.; Stevens, W. J. *J. Mol. Struct. (THEOCHEM)* **1995**, *338*, 303.
(28) Parr, R. G.; Yang, W. *Density-Functional Theory of Atoms and Molecules*; Oxford University Press: Oxford, U.K., 1989.
(29) Becke, A. D. *J. Chem. Phys.* **1993**, *98*, 5648.
(30) Boys, S. F.; Bernardi, F. *Mol. Phys.* **1970**, *19*, 553.
(31) Breneman, C. M.; Wiberg, K. B. *J. Comput. Chem.* **1990**, *11*, 367.
(32) *Gaussian94* and *Gaussian98* (*Revision A.6*); Gaussian, Inc.: Pittsburgh, PA, 1995 and 1998.

(33) *SYBYL6.2*; Tripoes Associates: St. Louis, MO, 1995.
(34) Kearney, P. C.; Mizoue, L. S.; Kumpf, R. A.; Forman, J. E.; McCurdy, A.; Dougherty, D. A. *J. Am Chem Soc.* **1993**, *115*, 9919.
(35) Deakyne, C. A.; Meot-Ner (Mautner), M. *J. Am. Chem. Soc.* **1985**, *107*, 474.
(36) Kim, S. K.; Lee, J. Y.; Lee, S. J.; Ha, T.-K.; Kim, D. H. *J. Am. Chem. Soc.* **1994**, *116*, 7399.
(37) Hoyau, S.; Norrman, K.; McMahon, T. B.; Ohanessian, G. *J. Am. Chem. Soc.* **1999**, *121*, 8864.
(38) Roelens, S.; Torriti, R. *J. Am. Chem. Soc.* **1998**, *120*, 12443.